DOI: 10.13009/EUCASS2019-879

On cup anemometers signal processing for better measurements and maintenance

Alvaro Ramos-Cenzano, Mikel Ogueta-Gutierrez and Santiago Pindado
Instituto Universitario de Microgravedad "Ignacio Da Riva" (IDR/UPM)
ETSI Aeronáutica y del Espacio, Universidad Politécnica de Madrid
Pza. del Cardenal Cisneros 3, Madrid 28040, Spain
alvaro.ramos.cenzano@alumnos.upm.es; mikel.ogueta@upm.es; santiago.pindado@upm.es

Abstract

The aerodynamics of rotatory elements is an extremely interesting topic that has brought attention of many researchers since the early works by Ludwig Prandtl. A clear example of rotational aerodynamics is the classic cup anemometer. In this research, anemometers equipped with opto-electronic output signal generators based on slotted wheels have been tested, their output signals being studied. The analysis of the output signal of the classic cup anemometer has a great relevance in the correct measurement of the wind speed. This correct analysis can help understand non-steady phenomena of the wind such as turbulence, optimize their maintenance, and also improve the study of the appropriate manufacture of the anemometers.

Slight deviations on cup anemometer wind speed measurements may lead to non-optimal policies in wind turbine's control, decreasing the economic revenue of the corresponding wind power plant. These deviations may be caused by two main different problems, among others. On the one hand, the processing method used to extract the rotation/output frequency if the sensor and, on the other hand, turbulence of the flow and measurement errors present in the slotted wheel of the opto-electronic output signal generator of the anemometer.

Two different processing methods to extract the aforementioned output frequency have been tested, namely the Fast Fourier Transform (FFT) and the counting pulses method (CP). These methods have been tested for different sampling frequencies and sampling time. The influence of the frequency is significant for both methods, but CP has been observed to have smaller residuals, especially at high sampling frequencies. The residuals have been observed to reach a constant value for both processing methods after a certain in value of the sampling frequency has been researched. Regarding sampling times, both methods decrease the residuals when the sampling time is increased, but the trend is more significant for CP.

Turbulence and other errors affect the signature (the train of pulses during one turn). The signature has been studied at very high sampling frequency (125 kHz). The tests have been performed in a wind tunnel under an ISO 17025 standard. Additional tests of the anemometer in still air and without cups have been performed. In those tests, the anemometer has been driven with a DC motor. Both cases have been compared analysing the first twelve Fourier harmonic terms.

1. Introduction

To this day, the cup anemometer remains the most used wind sensor within meteorology and wind power industries, despite the recent development of the actual sonic anemometer [1-6], such as SODAR [7-16]. Cup anemometers, before installation, require a thorough calibration process [17-20] regardless the use they are going to be given. In addition, it is important to mention that cup anemometers have certain limitations related to the inertial effects of the rotor in turbulent flows, causing the so-called "overspeeding" effect [21-26].

The output signal of some cup anemometers is analyzed to:

- Study the output frequency.
- Study the signature.

DOI: 10.13009/EUCASS2019-879

1.1 Output Frequency

The output frequencies studied, are generated by an opto-electronic system. This system consist of a slotted wheel fixed to the anemometers shaft and to an electronic device that registers led-generated light through the aforementioned wheel, generating to different voltage levels, being the higher one when the light reach the sensor, and the lower one when the sensor is not illuminated (see Figure 1).

As the cup anemometers output signal is square-wave, it is important to sample adequately the output system signal in order to extract an accurate value of the output frequency. In order to extract the aforementioned output frequency, two different procedures have been used, counting pulses (CP) and Fast Fourier Transformation (FFT), at different frequencies and time samplings.

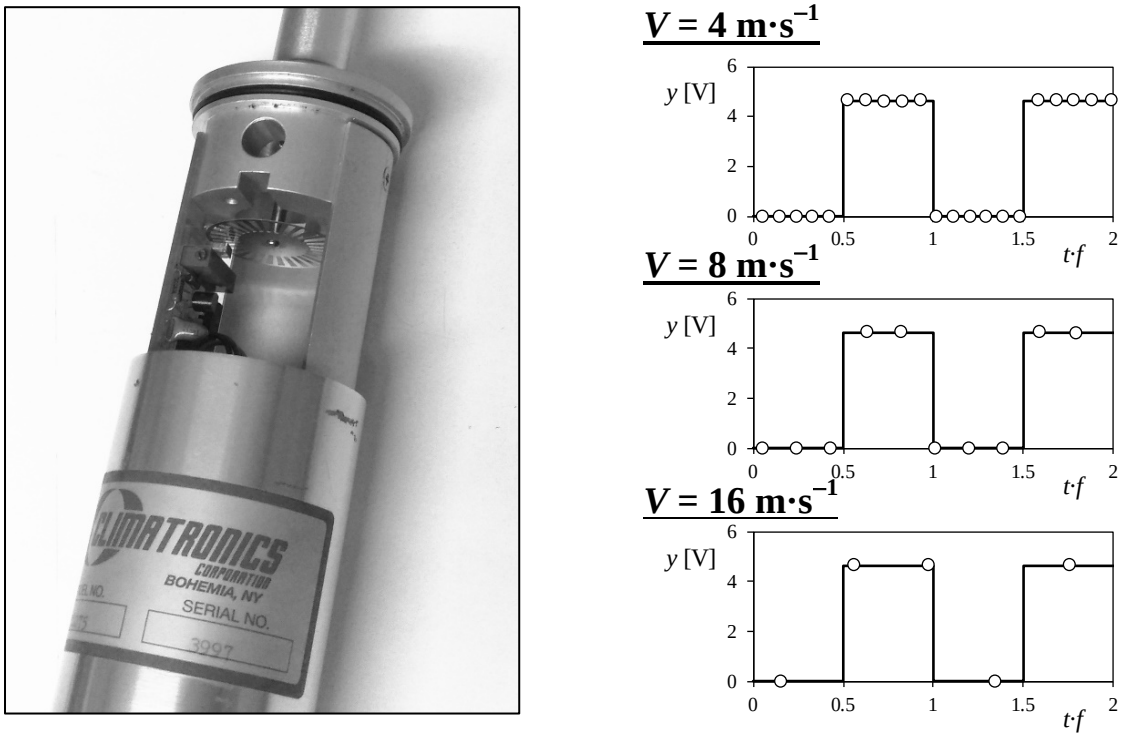

Figure 1: (Left) Opto-electronic output signal generator system of the Climatronics 100075 cup anemometer. (Right) Examples of sampling the analog square-wave output signal of a cup anemometer with the same sampling frequency al different wind speeds. The output voltage y is plotted in relation to the non-dimensional time $t \cdot f$ (where f is the anemometer´s output frequency). From [27].

1.2 Signature

The train of pulses during one turn is called the signature of the cup anemometer. These pulses are characteristics of each individual anemometer, as some differences among pulses might exist due to fabrication processes. Thanks to this train of pulses, is possible to study the cup anemometer´s performance by analyzing the changes in the signature along their life. The most accurate anemometers have from to 25 to 37 pulses per turn of the rotor. Thanks to this, the three accelerations of the rotor (and the corresponding decelerations) caused by the aerodynamics forces on each one of the cups the anemometers have (three cups) can be measured and analyzed, with the use of Fourier analysis [30-32].

DOI: 10.13009/EUCASS2019-879

2. Experimental Set-Up

2.1 Output Frequency

To proceed with output frequency extraction, firstly it is necessary a calibration process. The calibration was performed to five Thies Clima First-Class Advanced cup anemometers, following MEASNET procedures at LAC-IDR/UPM facilities [17]. The calibration is a wind tunnel testing of the anemometer in which a correlation between the frequency of the output signal of the anemometer and the wind-flow speed is carried out. To this case, thirteen measurement points between 4 m/s and 16 m/s are taken (13 measurement points), in order to define the cup anemometer transfer function through the calibration of constants A and B:

$$V = A \cdot f + B, \tag{1}$$

where V is the wind speed, which is calculated in relation to the output frequency of the anemometer, f, the slope, A and the offset, B, (see Figure 2). For each measurement point, samples with different time length (5, 10, 15, 20 and 25 seconds) were carried out at a frequency of 25 KHz. Data has been recorded with a National Instruments NI USB-6210 Data Acquisition System. Overall, 100 different calibrations for each individual cup anemometer, to analyze the effect of the following parameters:

- The way to extract the output frequency, comparing CP and FFT methods.
- The effects of the sampling frequency.
- The length of the data sample.

Table 1. Cases analyzed

Anemometers calibrated	• Anemometer-1 • Anemometer-2 • Anemometer-3 • Anemometer-4 • Anemometer-5	
Points per calibration	• 4 m·s^{-1} • 5 m·s^{-1} • 6 m·s^{-1} • 7 m·s^{-1} • 8 m·s^{-1} • 9 m·s^{-1} • 10 m·s^{-1}	• 11 m·s^{-1} • 12 m·s^{-1} • 13 m·s^{-1} • 14 m·s^{-1} • 15 m·s^{-1} • 16 m·s^{-1}
Length of samples	• 5 s • 10 s • 15 s • 20 s • 25 s	
Sampling frequencies analyzed	• 500 Hz • 625 Hz • 657.89 Hz • 675.98 Hz • 694.44 Hz • 714.29 Hz • 735.29 Hz • 757.58 Hz • 781.25 Hz • 806.45 Hz	• 833.33 Hz • 862.07 Hz • 892.86 Hz • 925.93 Hz • 961.54 Hz • 1000 Hz • 1250 Hz • 5000 Hz • 12500 Hz • 25000 Hz
Calculation of the output frequency, f	• CP (Counting Pulses) • FFT	

DOI: 10.13009/EUCASS2019-879

2.2 Signature

The signature studied corresponds to a *Climatronics 100075* cup anemometer. The study carried out for obtaining the aforementioned signature was, firstly in a wind tunnel (IDR/UPM calibration wind tunnel) [29, 34-36] and secondly, in still air. For this last case, a DC-motor geared to the anemometer has been used to rotate the anemometer (see Figure 2). The cup anemometer´s output signal was sampled at 20 KHz for the measurements in still air, initially. After, other set of measurements were carried out at 25 KHz, to check the possible effects of the sampling rate. For the wind tunnel tests, the tests were carried out at a larger sampling frequency (125 kHz). This larger frequency was selected to obtain new insights into the effect of the turbulence on the anemometer´s performance.

Figure 2: Testing set-up for measuring the Climatronics 100075 cup anemometer signature in still air.

3. Results

3.1 Analysis of the Output Frequency Extraction Procedure on the Cup Anemometer Performance

The transfer function of the first anemometer calibrated can be seen in Figure 3 (solid line). In that figure, the results for the 500 Hz sampling frequency and 1000 Hz sampling frequency are displayed, with a sampling time of 25 s. The samples carried out have been done at frequencies of 500 and 1000 Hz, with a time length of 25 seconds. It can be observed the results for the sampling frequency of 1000 Hz are in good agreement with the transfer function obtained in the IDR/UPM calibration, which followed ISO 17025 and MEASNET standards are quite accurate compared with the ones from IDR/UPM calibration, whereas, at 500 Hz, the results present problems for wind speeds above 11 m/s. This happens because the sampling frequency is not enough to correctly capture the square-wave generated by the opto-electronic system. Therefore, according to Nyquist theorem [28], at 12 m/s (or larger wind velocities) low sampling frequencies are not trustworthy and higher sampling frequencies should be selected in order to extract properly the output frequency.

DOI: 10.13009/EUCASS2019-879

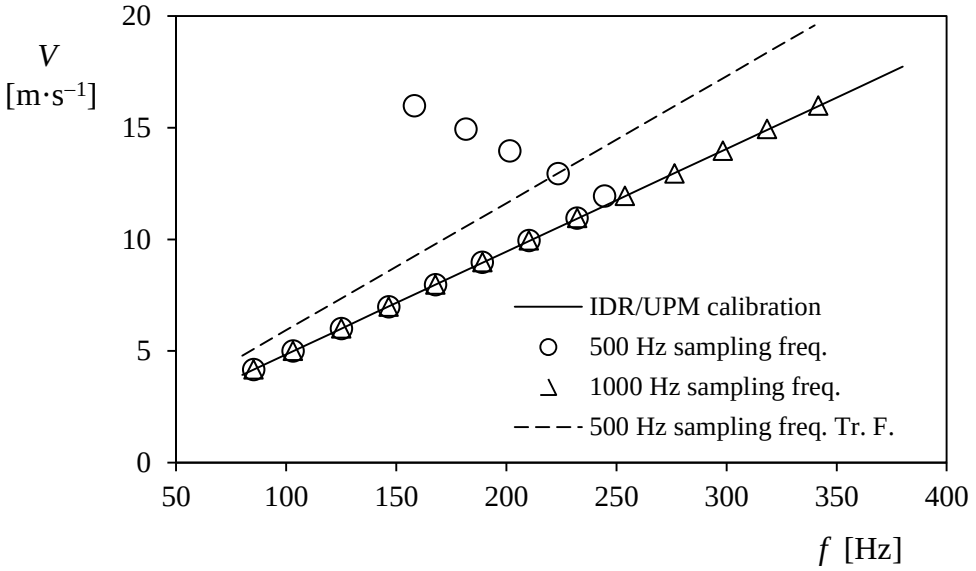

Figure 3: Anemometer-1/25-second 500 and 1000 Hz datasets. Points (output frequencies) extracted by CP. IDR/UPM reference calibration, i.e., transfer function of Anemometer-1 has been included (solid line). The transfer function (Tr. F.) based on the Anemometer-1/25-second 500 Hz dataset is also included (dashed line)

The accuracy of the transfer functions calculated in the different conditions is easily evaluated by calculating the residuals. The residuals in these cases, are defined as the wind speed differences between the testing wind speeds, V_i, and the ones from the transfer function at the calculated output frequencies, f_i (see Figure 4):

$$r_{s,i} = V_i - (A \cdot f_i + B). \tag{2}$$

An alternative way to estimate the accuracy of the calculated transfer functions has been also done. The wind speed error is calculated as the difference between the velocity calculated with the IDR/UPM calibration and the one calculated with the estimated transfer function (see Figure 5):

$$\Delta V_i = (A^* \cdot f_i + B) - (A \cdot f_i + B). \tag{3}$$

In addition, the averaged value of the residuals, R_S, and the averaged percentage value of the wind speed error, ΔV_{avg}, are calculated to characterize the accuracy of the transfer functions corresponding to all analyzed different sampling rate datasets:

$$R_S = \frac{1}{13}\sum_{i=1}^{13}|r_{s,i}|, \tag{4}$$

$$\Delta V_{avg} = \frac{1}{13}\sum_{i=1}^{13}\frac{|\Delta V_i|}{(A^* \cdot f_i + B^*)}. \tag{5}$$

In Figures 6 and 7, the decreasing trends of both the residuals and the wind speed error in relation to the sampling frequency can be observed. The residuals and the wind speed error reach a constant value at sampling frequencies around 700 Hz. The results obtained by CP are better as the show lower values when compared to the ones obtained by FFT, but the frequency at which they reach those values is a bit higher. Finally, from the results, it can be deduced that the error depends on the wind speed (output frequency). The relationship between the errors and the variable (output frequency or wind speed) is similar to a first order transfer function.

DOI: 10.13009/EUCASS2019-879

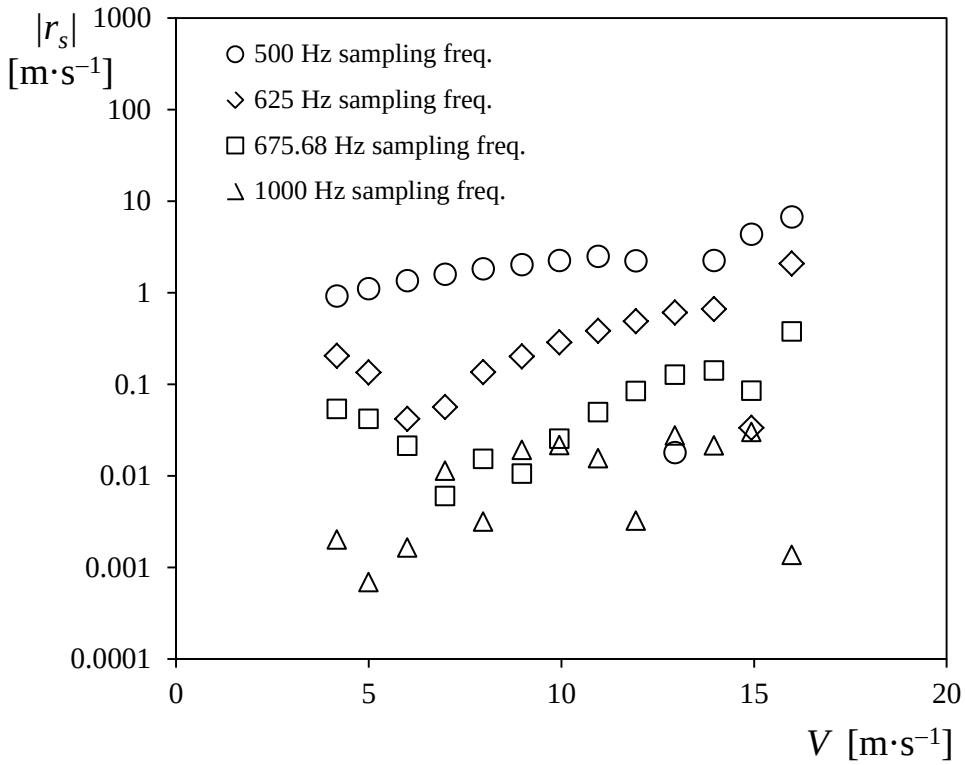

Figure 4: Anemometer-1/25-second 500, 625, 675.68, and 1000 Hz datasets. Absolute values of the transfer functions residuals, r_S, calculated by CP.

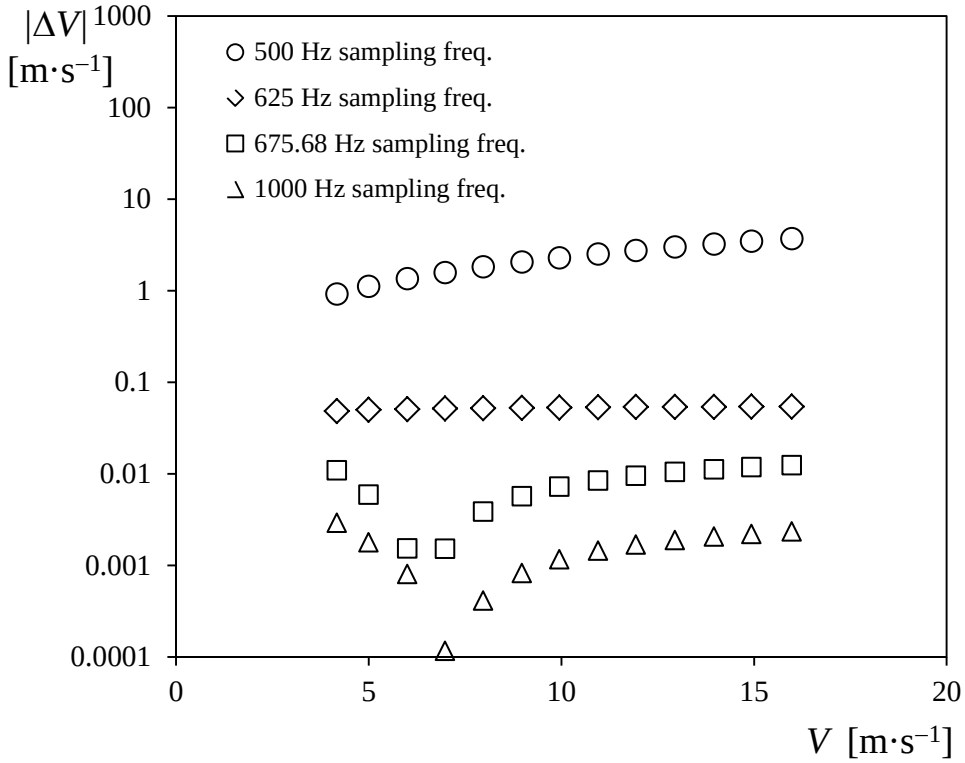

Figure 5: Anemometer-1/25-second 500, 625, 675.68, and 1000 Hz datasets. Absolute values of the wind speed error,ΔV, calculated by CP.

DOI: 10.13009/EUCASS2019-879

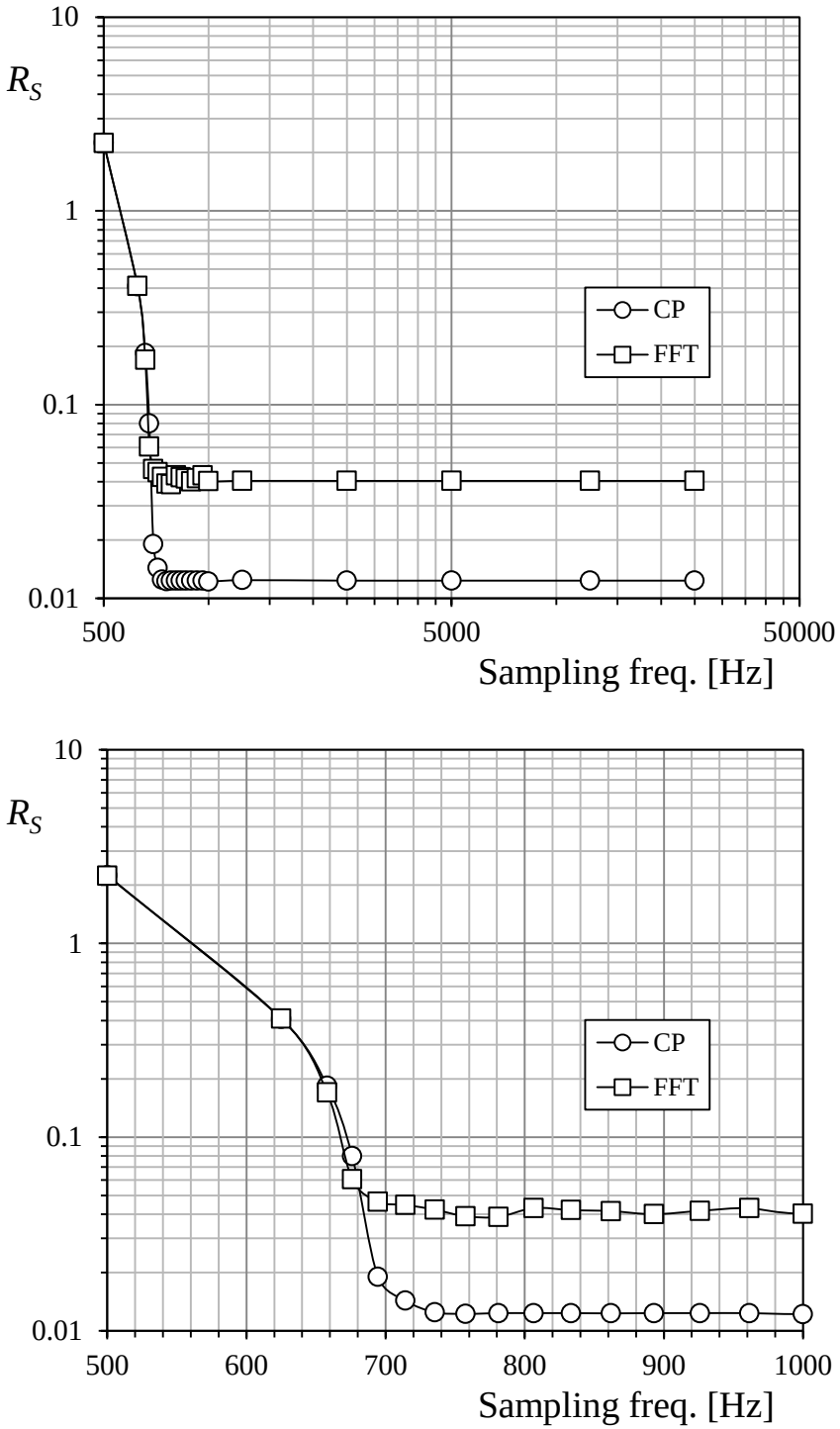

Figure 6: Anemometer-1/25-second datasets. Averaged value of the transfer functions residuals, R_S, in relation to the sampling frequency. The residuals were calculated by CP and by using the FFT. On the left, all results are displayed, whilst on the right, only the results for frequencies from 500 Hz to 1000 Hz are displayed.

DOI: 10.13009/EUCASS2019-879

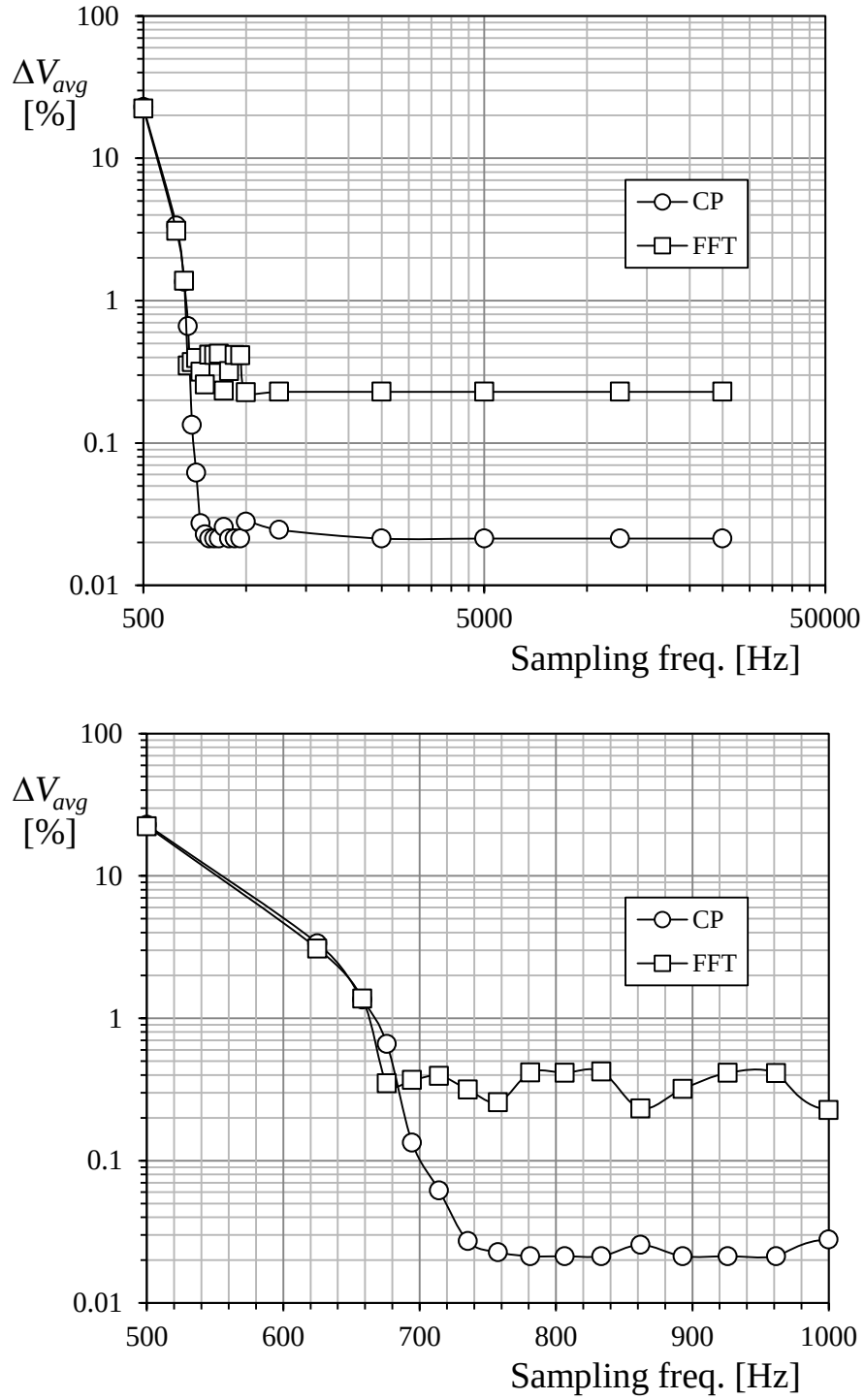

Figure 7: Anemometer-1/25-second datasets. Averaged value of the transfer functions wind speed error, ΔV_{avg}, in relation to the sampling frequency. The residuals were calculated by CP and by using FFT. On the left, all residuals are displayed, whilst on the right, only the results for frequencies from 500 Hz to 1000 Hz are displayed.

DOI: 10.13009/EUCASS2019-879

3.2 Study on the Cup Anemometer's Signature

The evolution of the frequency in one lap can be studied by the Fourier analysis. The Fourier analysis leads to the following expression:

$$\omega(t) = \omega_0 + \sum_{n=1}^{\infty} A_n \sin(n\omega_0 t + \varphi_n). \quad (6)$$

Ideally, only the term related to ω_0 and the harmonic terms multiple of three should appear (because of the three accelerations of the three cups in the lap). However, in reality all the terms are present, even though many of them are not significant. The pulse length, d_p, of the analysed cup anemometer with regard to the pulse number is shown in figure 8 for wind tunnel speeds of 2, 4, 6 and 8 m/s. The 3 accelerations of the rotor due to the 3-cup configuration can be clearly observed. Also the 9-term Fourier approximation to the pulse length at 2 m/s is included in the graph to show the accuracy of this mathematical tool.
If the terms related to the acceleration of the three cups (the multiples of three in the Fourier analysis) can be subtracted, the effect of the mechanism of each anemometer can be studied. This is interesting in order to comprehend the influence of manufacture or maintenance differences in the performance of the anemometer, and its effect can be taken into account to obtain a better performance.

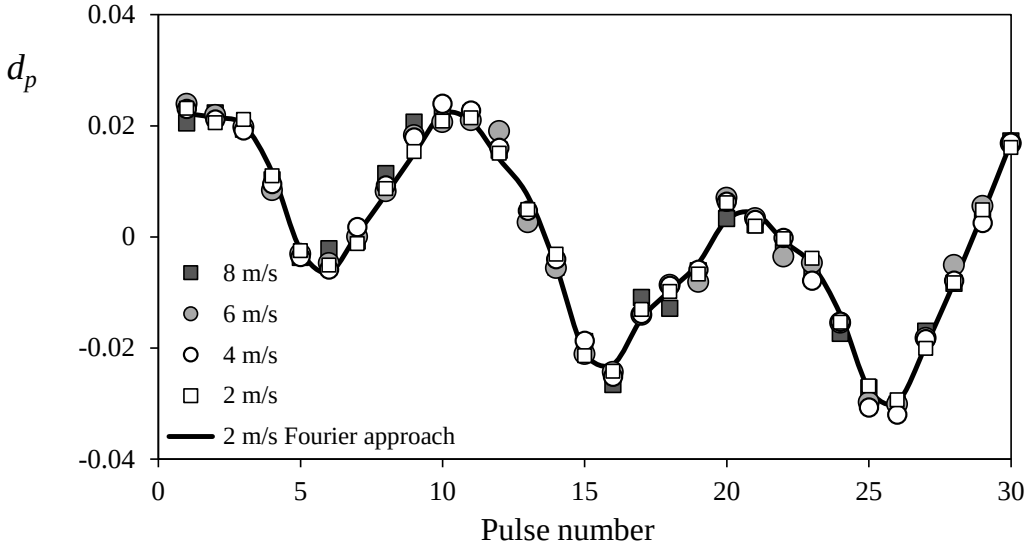

Figure 8: Pulse length data of the Climatronics 100075 cup anemometer recorded at 2, 4, 6 and 8 m/s. A 9-term Fourier approximation to the 2 m/s data is also included in the graph.

DOI: 10.13009/EUCASS2019-879

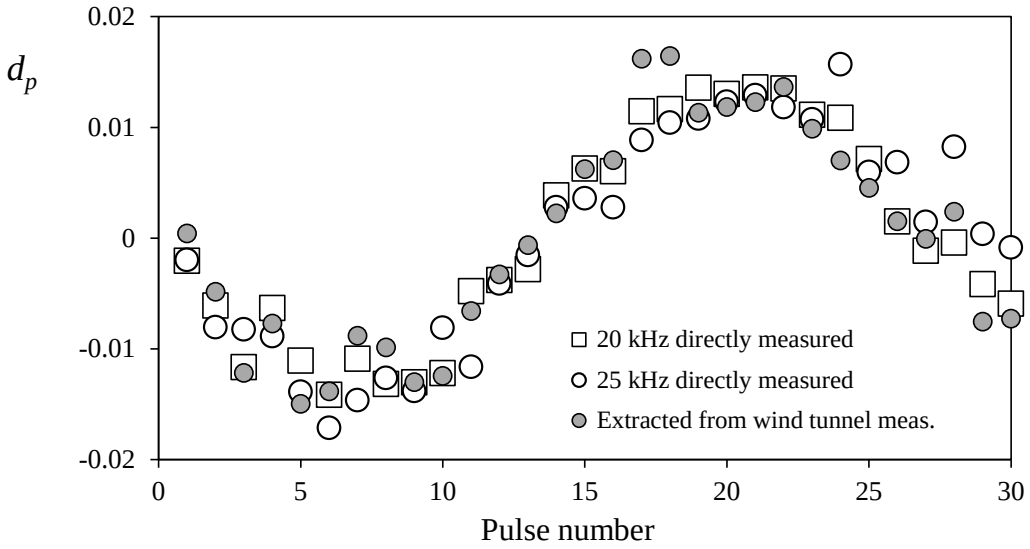

Figure 9: Signature of the Climatronics 100075 cup anemometer directly measured (see Figure 3) at 20 kHz and 25 kHz. The indirect signature extracted with the data recorded in wind tunnel at 2 m/s is also included in the graph.

In Figure 9 Climatronics 100075 cup anemometer signature is shown, which has been directly measured (outside the wind tunnel) at 20 and 25 kHz, and in the wind tunnel. The signature is presented as the percentage length of each one of the 30 pulses per turn of the slotted wheel, in relation to the average length of the pulses, d_p (1/30 of the total turn). It is also easy to appreciate a sinusoidal pattern, indicating a displacement of the pulse wheel center from the rotation axis of the anemometer shaft. The terms of the Fourier analysis are displayed in Figure 10. These results are in good agreement with the results from Figure 9, where the first harmonic term is the most relevant one.
The signature obtained from the output of the anemometer at 2 m/s has also been added to the signatures directly measured. It is clear that the first term of the Fourier analysis is very similar, and that the third term, due to the acceleration of the cups, is only present in the measurements performed in the wind tunnel (in still air, the cups have been removed, see figure 2). The results indicate the possibility of extracting a cup anemometer signature from a calibration process and not using a specific procedure in still air in accordance with the work developed by Dalberg et al. [33]. This is a very interesting result, since the signature can be taken into account to improve the performance of the anemometer.

DOI: 10.13009/EUCASS2019-879

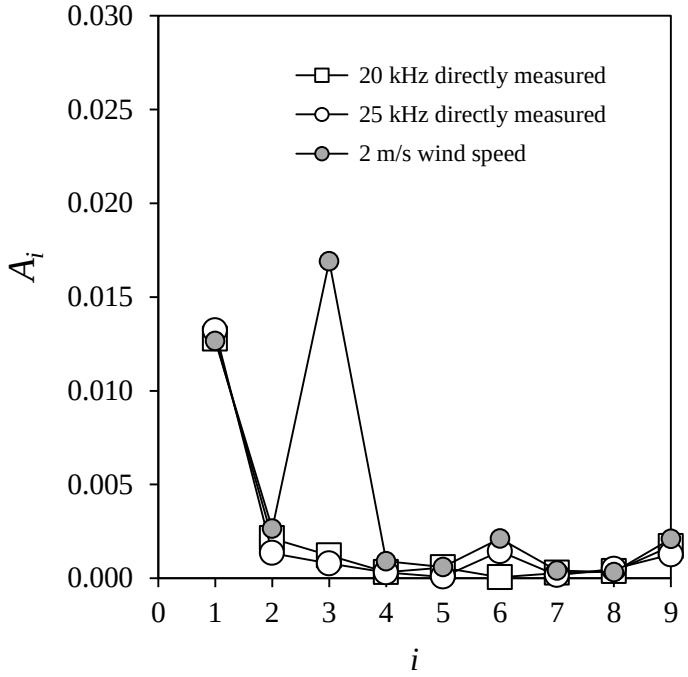

Figure 10. First nine harmonic terms, A_i, from signature of Climatronics 100075 cup anemometer directly measured. The harmonic terms from the pulse length data recorded at 2 m/s is also included in the graph.

4. Conclusions

The most relevant conclusions of the present work are:

- Counting pulses (CP) has proven to be the better way to extract the output frequency when compared to FFT. The error of calibrations based on the latter being within ±0.4% bracket (for values large enough of both the dataset and the measurement frequency).
- Larger samples increase the accuracy of the transfer function. Nevertheless, it seems that this accuracy remains within a stabilized range for sample lengths larger than 20 seconds.
- Results suggest that sampling frequencies larger than 781.25 Hz are required to measure the output frequency of Thies Clima First-Class Advanced during MEASNET calibration procedure. This requirement should change for other cup anemometers with different number of square pulses per turn
- The results indicates the possibility of extracting cup anemometer signature indirectly (Which is unique for each single anemometer equipped with opto-electronic output signal generator) during the calibration of the wind speed sensor. Therefore, it facilitates the use of the signature to filter the cup anemometer´s output signal in order to increase the accuracy of this wind speed sensor.

References

[1] Cutler N J, Outhred H R and MacGill I F 2012 Using nacelle-based wind speed observations to improve power curve modeling for wind power forecasting *Wind Energy* **15** 245–58

[2] Wagner R, Pedersen T F, Courtney M, Antoniou I, Davoust S and Rivera R L 2013 Power curve measurement with a nacelle mounted lidar *Wind Energy* **20** n/a-n/a

[3] Mikkelsen T, Angelou N, Hansen K, Sjöholm M, Harris M, Slinger C, Hadley P, Scullion R, Ellis G and Vives G 2013 A spinner-integrated wind lidar for enhanced wind turbine control *Wind Energy* **16** 625–43

[4] Pedersen T F, Demurtas G and Zahle F 2015 Calibration of a spinner anemometer for yaw misalignment

measurements *Wind Energy* **18** 1933–52

[5] St. Martin C M, Lundquist J K, Clifton A, Poulos G S and Schreck S J 2016 Atmospheric turbulence affects wind turbine nacelle transfer functions *Wind Energy Sci. Discuss.* 1–22

[6] Demurtas G, Friis Pedersen T and Wagner R 2017 Nacelle power curve measurement with spinner anemometer and uncertainty evaluation *Wind Energy Sci.* **2** 97–114

[7] Lang S and McKeogh E 2011 LIDAR and SODAR Measurements of Wind Speed and Direction in Upland Terrain for Wind Energy Purposes *Remote Sens.* **3** 1871–901

[8] Wagner R, Courtney M, Gottschall J and Lindelöw-Marsden P 2011 Accounting for the speed shear in wind turbine power performance measurement *Wind Energy* **14** 993–1004

[9] Bradley S 2013 Aspects of the Correlation between Sodar and Mast Instrument Winds *J. Atmos. Ocean. Technol.* **30** 2241–7

[10] Sanz Rodrigo J, Borbón Guillén F, Gómez Arranz P, Courtney M S, Wagner R and Dupont E 2013 Multi-site testing and evaluation of remote sensing instruments for wind energy applications *Renew. Energy* **53** 200–10

[11] Hasager C, Stein D, Courtney M, Peña A, Mikkelsen T, Stickland M and Oldroyd A 2013 Hub Height Ocean Winds over the North Sea Observed by the NORSEWInD Lidar Array: Measuring Techniques, Quality Control and Data Management *Remote Sens.* **5** 4280–303

[12] Suomi I and Vihma T 2018 Wind gust measurement techniques—From traditional anemometry to new possibilities *Sensors (Switzerland)* **18** 1–27

[13] Mikkelsen T 2014 Lidar-based Research and Innovation at DTU Wind Energy – a Review *J. Phys. Conf. Ser.* **524** 012007

[14] Frehlich R and Sharman R 2004 Estimates of Turbulence from Numerical Weather Prediction Model Output with Applications to Turbulence Diagnosis and Data Assimilation *Mon. Weather Rev.* **132** 2308–24

[15] Towers P and Jones B L 2016 Real-time wind field reconstruction from LiDAR measurements using a dynamic wind model and state estimation *Wind Energy* **19** 133–50

[16] Willis D J, Niezrecki C, Kuchma D, Hines E, Arwade S R, Barthelmie R J, DiPaola M, Drane P J, Hansen C J, Inalpolat M, Mack J H, Myers A T and Rotea M 2018 Wind energy research: State-of-the-art and future research directions *Renew. Energy* **125** 133–54

[17] Pindado S, Vega E, Martínez A, Meseguer E, Franchini S and Pérez I 2011 Analysis of calibration results from cup and propeller anemometers. Influence on wind turbine Annual Energy Production (AEP) calculations *Wind Energy* **14** 119–32

[18] Pindado S, Barrero-Gil A and Sanz A 2012 Cup Anemometers' Loss of Performance Due to Ageing Processes, and Its Effect on Annual Energy Production (AEP) Estimates *Energies* **5** 1664–85

[19] Pindado S, Sanz A and Wery A 2012 Deviation of Cup and Propeller Anemometer Calibration Results with Air Density *Energies* **5** 683–701

[20] Vega E, Pindado S, Martínez A, Meseguer E and García L 2014 Anomaly detection on cup anemometers *Meas. Sci. Technol.* **25** 127002 (6pp)

[21] Wyngaard J C, Bauman J T and Lynch R A 1974 Cup anemometer dynamics *Flow Its Meas. Control Sci. Ind.* **1** 701–8

[22] Busch N E and Kristensen L 1976 Cup anemometer overspeeding *J. Appl. Meteorol.* **15** 1328–1332

[23] Wyngaard J C 1981 Cup, propeller, vane, and sonic anemometers in turbulence research *Annu. Rev. Fluid Mech.* **13** 399–423

[24] Westermann D 1996 Overspeeding - über das eigentümliche Tiefpaßverhalten von Schalensternanemometern (Overspeeding measurements of cup anemometers) *DEWI Mag.* **9** 56–63

[25] Kristensen L 2000 Measuring Higher-Order Moments with a Cup Anemometer *J. Atmos. Ocean. Technol.* **17** 1139–48

[26] Kristensen L, Jensen G, Hansen A and Kirkegaard P 2001 *Field Calibration of Cup Anemometers. Risø–R–1218(EN)* (Roskilde, Denmark)

[27] Vidal-Pardo A and Pindado S 2018 Design and Development of a 5-Channel Arduino-Based Data

DOI: 10.13009/EUCASS2019-879

Acquisition System (ABDAS) for Experimental Aerodynamics Research *Sensors* **18** 1–20

[28] Nyquist H 1928 Certain Topics in Telegraph Transmission Theory *Trans. Am. Inst. Electr. Eng.* **47** 617–44

[29] S. Pindado, E. Vega, A. Martínez, E. Meseguer, S. Franchini, I. Pérez, Analysis of calibration results from cup and propeller anemometers. Influence on wind turbine Annual Energy Production (AEP) calculations, Wind Energy. 14 (2011) 119–132.

[30] S. Pindado, J. Cubas, F. Sorribes-Palmer, On the harmonic analysis of cup anemometer rotation speed: A principle to monitor performance and maintenance status of rotating meteorological sensors, Measurement. 73 (2015) 401–418.

[31] E. Vega, S. Pindado, A. Martínez, E. Meseguer, L. García, Anomaly detection on cup anemometers, Meas. Sci. Technol. 25 (2014) 127002 (6pp).

[32] A. Martínez, E. Vega, S. Pindado, E. Meseguer, L. García, Deviations of cup anemometer rotational speed measurements due to steady state harmonic accelerations of the rotor, Measurement. 90 (2016) 483–490.

[33] J.-Å. Dahlberg, T.F. Pedersen, P. Busche, ACCUWIND -Methods for Classification of Cup Anemometers. Risø-R-1555(EN), Roskilde, Denmark, 2006.

[34] S. Pindado, J. Pérez, S. Avila-Sanchez, On cup anemometer rotor aerodynamics, Sensors. 12 (2012) 6198–6217.

[35] S. Pindado, I. Pérez, M. Aguado, Fourier analysis of the aerodynamic behavior of cup anemometers, Meas. Sci. Technol. 24 (2013) 065802 (9 pp).

[36] S. Pindado, J. Cubas, F. Sorribes-Palmer, The Cup Anemometer, a Fundamental Meteorological Instrument for the Wind Energy Industry. Research at the IDR/UPM Institute, Sensors. 14 (2014) 21418–21452.